

# Ultra-Wideband Transient Arrays: Focusing and Defocusing

Shaya Karimkashi<sup>1</sup>, and Ahmed A. Kishk<sup>2</sup>

<sup>1</sup>*Advanced Radar Research Center, National Weather Center  
Norman, OK, USA*

Shaya.karimkashi@ou.edu

<sup>2</sup>*Department of Electrical & Computer Engineering, Concordia University  
Montreal, CA  
kishk@ece.concordia.ca*

**Abstract**—Some focusing properties of the ultra-wideband time-domain focused array antennas were presented. Large current radiators are considered as the elements of the antenna array. Several antenna arrays with different sizes and number of elements are modeled. It is shown that similar to narrow band antennas, the actual maximum field region shifts from the intended focus region towards the antenna aperture.

## I. INTRODUCTION

Focused array antennas based on Ultra-Wide-Band (UWB) impulse waveforms can provide high concentration of electromagnetic energy into small regions by controlling the timing of pulses radiated by each element [1-6]. Higher performance compared to narrowband arrays [7-12] can be achieved in terms of higher angular resolution and increasing the peak power delivered to the focused region. These antennas are of interest in medical applications, radar, homeland security systems and communication systems.

The Large Current Radiator (LCR) is considered as the array element. An LCR consists of a generator, a closed loop and a ferrite plate. The LCR is inherently a non-resonating structure and thus permits to radiate electromagnetic (EM) waves with either sinusoidal or non-sinusoidal time variation [13-15]. In order to model the mutual coupling between the LCR elements within the array, the infinitesimal dipole array modeling is considered. Using this method, each LCR is replaced by a set of infinitesimal dipoles producing the same electromagnetic fields as the LCR [16-19].

The main goal of this paper is to study some focusing and defocusing behavior of time-domain UWB focused arrays. The mutual coupling between the LCR elements is obtained using the reaction theorem [20-22]. It should be noted that LCR elements can be spaced at distances larger than the spatial duration of the pulse to ignore the mutual coupling as well as multiple scattering effects between the elements. However, using the IDMs concept, the array can be modeled by assuming any spacing between the elements. Using this model, several antenna arrays are modeled while the coupling between the elements is included.

## II. LARGE CURRENT RADIATOR AND ITS MODELING

### A. Large Current radiator (LCR)

The Large Current Radiator (LCR) is considered as the array element. Fig. 1 shows the configuration of an LCR consisting of a generator, a closed loop and a ferrite plate. The LCR is inherently a non-resonating structure and thus permits to radiate electromagnetic (EM) waves with either sinusoidal or non-sinusoidal time variation. Fig. 1 shows the schematic of an LCR. In order to model the LCR with the ferrite plate, only the radiator part is modeled while the backward radiation is ignored because of the presence of the ferrite plate. The LCR is excited by a Gaussian pulse with different variances.

### B. Infinitesimal Dipole Modeling

A set of infinitesimal dipoles (electric or magnetic), representing an actual antenna, can be obtained by using an optimization algorithm to minimize the difference between the near field of the dipoles and those of the actual antenna. Each dipole is represented by seven parameters: the position of the elements (x, y, z coordinates); the complex dipole moment (the real and imaginary part), and its orientation ( $\theta$  and  $\phi$ ). It should be mentioned that the dipole locations are limited within the volume of the actual antenna. The near-field is computed on a square observation plane with side lengths of 1000 mm located at a distance 500 mm from the antenna aperture. The near field is computed at 60 frequency points from 50 MHz to 3GHz. The total number of samples is 121 points at each frequency. The modified invasive weed optimization (IWO) algorithm with restricted boundary condition is applied to determine the moment, the position, and the orientation of the dipoles. The total number of 30 electric dipoles is obtained after the optimization. The frequency domain solution of the problem is used and converted to the time domain using the inverse Fourier transform. In other words, by knowing the frequency response of the LCR, which is the summation of electric or magnetic fields of all the dipoles, and the frequency components of the Gaussian pulse, the output radiation patterns in the frequency domain are obtained.

### III. FOCUSED ARRAY ANTENNAS

#### A. $4 \times 4$ LCR Array

A two-dimensional square array composed of 16 ( $4 \times 4$ ) elements, shown in Fig. 2, is considered. The array elements are uniformly spaced in the  $xz$ -plane with separation of  $d = 0.3$  m between elements. Each LCR element, replaced by a set of dipoles, is excited by a Gaussian pulse. Therefore, there is an equally weighted amplitude distribution for the array. The array antenna can focus the radiated pulses by setting a proper delay time at each element. Therefore, the radiating waves arrive simultaneously and add up in phase at the desired focusing point. For a focusing distance  $F$  from the antenna aperture the time delay of  $i$ -th element should be set up as

$$t_i = \frac{\sqrt{F^2 + L_i^2}}{c} \quad (1)$$

where  $c$  is the speed of light and  $L_i$  is the distance of the  $i$ -th element form the center of the square aperture. The radiation near field pattern of the array at the focal distance from the aperture at time  $t$  can be obtained by the summation of the radiated fields of all elements. However, the coupling between the elements is included by using the IDM technique. Observing the field variations at several different time instances (Fig. 2a), we can see that a higher intensity value occurs at a point closer to the antenna aperture compared to the focal point. The bold line in Fig. 2a shows the field at the time instance  $t = 1.2m/c$ . The variation of peak power values for different time instances are shown in Fig. 2b. It can be seen that the maximum intensity occurs at a point closer to the antenna aperture.

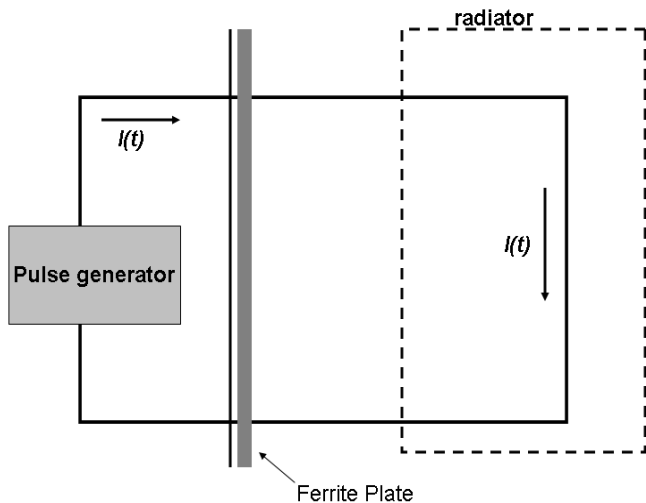
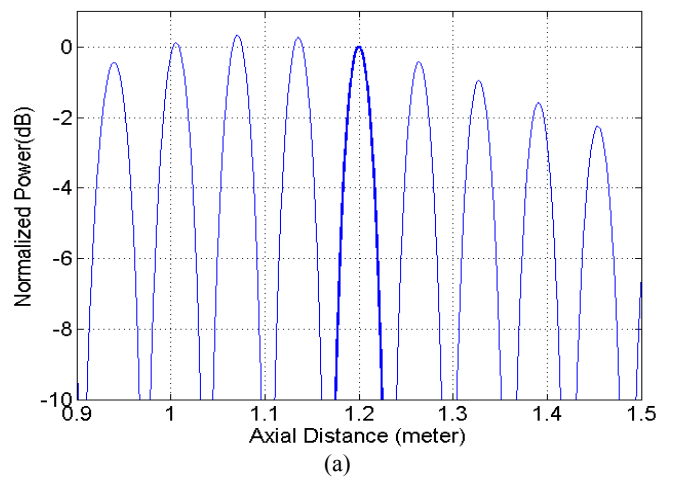


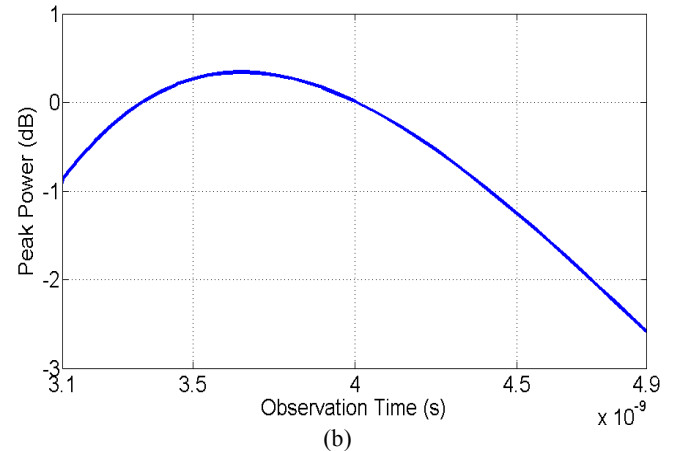
Fig.1. The schematic of an LCR.

#### B. $8 \times 8$ LCR Array

In this section, a larger array antenna composed of 64 ( $8 \times 8$ ) elements is considered. The elements are separated by  $d = 0.3$  m and a Gaussian pulse excites each element. The antenna is designed to have a focal length of 4.8 m. Fig. 3a shows the variation of the normalized power versus the axial distance at  $t = F/c$  instance. The variation of the power distribution versus the axial distance for different time instances is shown in Fig. 3b. The bold line shows the field at the time instance  $t = F/c$ . It can be seen that the maximum intensity occurs at  $y = 4.48$  m from the antenna aperture. The variation of the peak power versus the different time instances for the  $8 \times 8$  array is shown in Fig. 3c. It can be seen that by increasing the focal length the focal shift has been increased.



(a)



(b)

Fig. 2.  $4 \times 4$  uniformly spaced array (a) normalized field distribution versus the axial distance at different time instances. The bold line shows the field at the time instance  $t = F/c = 4$  (ns) (b) the variation of peak power values for different time instances.

In order to further study the behavior of the focal shift, the  $8 \times 8$  array antenna with many different focal lengths is modeled. Fig. 3 depicts the variations of the maximum intensity length and the difference between the power values at the focal point and maximum intensity point for different focal lengths of the  $8 \times 8$  array antenna. It can be seen that similar to narrow band antennas, for the focal point close to the antenna aperture, the maximum intensity is very close to the focal point, but as the focal point moves away from the antenna aperture, the focal shift increases.

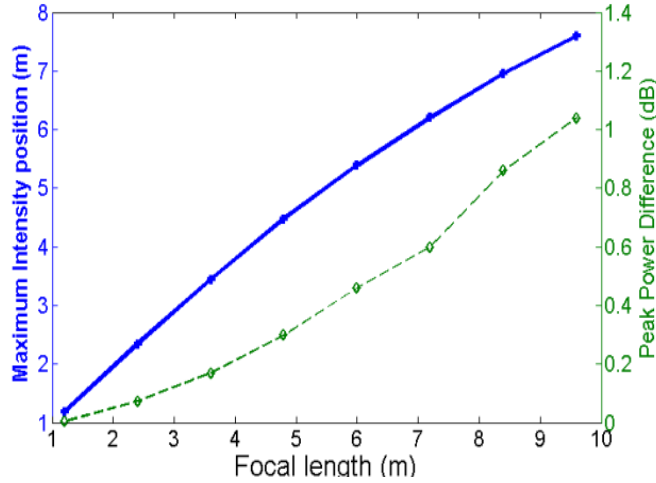


Fig.3. The variation of the maximum intensity point (Solid) and peak power difference (dash) versus the focal length of the  $8 \times 8$  array antenna.

#### IV. CONCLUSION

Some new focusing properties of time-domain ultra wide band (UWB) focusing array antennas were presented. The large current radiator (LCR) was considered as the UWB antenna element. Each LCR was replaced by a set of infinitesimal dipoles modeling both the near field and the far field patterns of the antenna element and the coupling between the elements. Calculating the variation of the power distributions versus the axial length at different time instances showed the focal shift effect in the near-field pattern. It was shown that the maximum intensity occurred at a point closer to the antenna aperture than the focal distance and this displacement was increased as the focal point moved away from the antenna aperture. It was shown that this displacement can only be seen when the radiated pulse is observed at successive time instants.

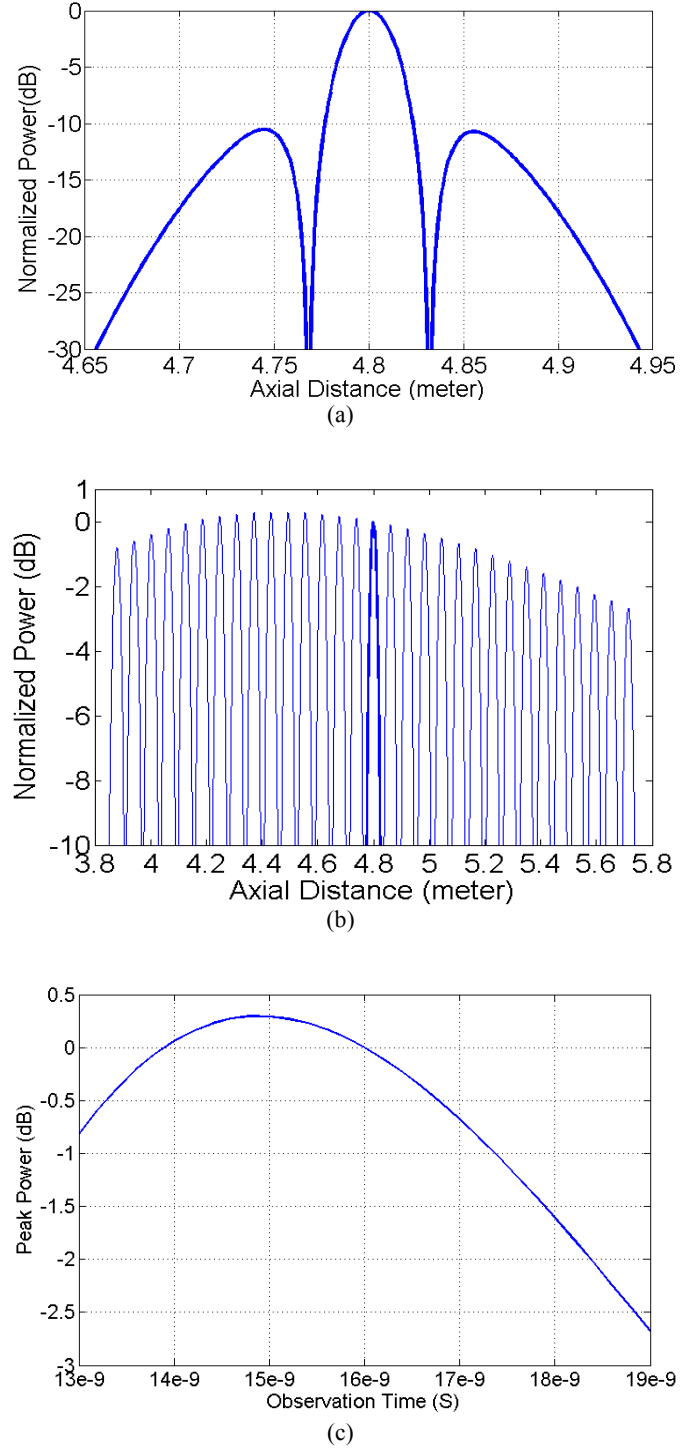


Fig. 4. The  $8 \times 8$  array antenna with  $F = 4.8$  m (a) the variation of the normalized power pattern versus the axial distance. (b) the variation of the near field pattern versus the axial length at different time instances. The bold line shows the field at the time instance  $t = F/c = 16$  (ns). (c) The variation of the peak power versus the different time instances at the focal point.

## REFERENCES

- [1] D. R. Hackett, C. D. Taylor, D. P. Mclemore, H. Dogliani, W. A. Walton, and A. J. Leyendecker, "A transient array to increase the peak power delivered to a localized region in space: Part I—theory and modeling," *IEEE Trans. Antennas Propag.*, vol. 50, no. 12, pp. 1743–1750, Dec. 2002.
- [2] S. Jacobsen, "Reduction of hot spots in hyperthermia by means of broadband energy transmission," *Electron. Lett.*, vol. 34, no. 20, p. 1901–1902, Oct. 1998.
- [3] M. C. Converse, E. J. Bond, S. C. Hagness, and B. D. Van Veen, "Ultrawide-band microwave space-time beamforming for hyperthermia treatment of breast cancer: A computational feasibility study," *IEEE Trans. Microw. Theory Tech.*, vol. 52, no. 8, p. 1876–1889, Aug. 2004.
- [4] M. Converse, E. J. Bond, B. D. Van Veen, and S. Hagness, "A computational study of ultra-wideband versus narrowband microwave hyperthermia for breast cancer Treatment," *IEEE Trans. Microw. Theory Tech.*, vol. 54, no. 5, p. 2169–2180, May 2006.
- [5] C. E. Baum et al., "Transient Arrays," in *Ultra-Wideband, Short-Pulse Electromagnetics 3*, New York, Plenum, 1997, p. 129–138.
- [6] M. G. M. Hussain, "Characteristics of ultra-wideband electromagnetic missiles generated by focused two-dimensional array," *Progr. Electromagn. Res.*, vol. 49, p. 143–159, 2004.
- [7] J. W. Sherman, "Properties of focused aperture in the Fresnel region," *IRE Trans. Antennas Propagat.*, Vols. AP-10, no. 4, pp. 399–408, 1962.
- [8] R. C. Hanson, "Focal region characteristics of focused array antennas," *IEEE Trans. Antennas Propagat.*, Vols. AP-33, no. 6, pp. 1328–1337, 1985.
- [9] W. J. Graham, "Analysis and synthesis of axial field patterns of focused apertures," *IEEE Trans. Antennas Propagat.*, Vols. AP-31, no. 4, pp. 665–668, 1983.
- [10] S. Karimkashi and A. A. Kishk, "A new Fresnel zone antenna with beam focused in the Fresnel region," in *URSI National Radio Science Meeting*, Chicago, 2008.
- [11] S. Karimkashi and A. A. Kishk, "Focused microstrip array antenna using a Dolph-Chebyshev near-field design," *IEEE Trans. Antennas Propag.*, Vols. vol. 57, no. 12, pp. no. 12, p. 3813–3820, Dec. 2009..
- [12] S. Karimkashi, A. A. Kishk, "Focusing Properties of Fresnel Zone Plate Lens Antennas in the Near-Field Region," *IEEE Trans. Antennas Propag.*, vol. 59, no. 5, pp. 1481–1487, May 2011.
- [13] H. F. Harmuth, N. J. Mohamed, "Large-current radiators," *IEE Proceedings-H*, vol. 139, no. 4, Aug. 1992.
- [14] G. P. Pochanin, P. V. Kholod, and S. A. Masalov, "Large current radiator with S-Diode Switch," *IEEE Trans. Electromagn. Compat.*, vol. 43, no. 1, pp. 94–100, 2001.
- [15] G. P. Pochanin, and S. A. Masalov, "Use of the coupling between elements of the vertical antenna array of LCRs to gain radiation efficiency for UWB pulses," *IEEE Trans. Antennas Propagat.*, vol. 55, no. 6, pp. 1754–1759, Jun. 2007
- [16] S. M. Mikki and A. A. Kishk, "Theory and applications of infinitesimal dipole models for computational electromagnetics," *IEEE Trans. Antennas Propag.*, vol. 55, p. 1325–1337, 2007.
- [17] X. H. Wu, A. A. Kishk, and A. W. Glisson, "A transmission line method to compute the far-field radiation of arbitrary Hertzian dipoles in a multilayer structure embedded with PEC strip interfaces," *IEEE Trans. Antennas Propag.*, vol. 55, p. 3191–3198, Nov. 2007.
- [18] X. H. Wu, A. A. Kishk, and A. W. Glisson, "A transmission line method to compute the far-field radiation of arbitrarily directed Hertzian dipoles in a multilayer dielectric structure: Theory and applications," *IEEE Trans. Antennas Propag.*, vol. 54, pp. 2731–2741, Oct. 2006.
- [19] X. H. Wu, A. A. Kishk, and A. W. Glisson, "Modeling of wide band antennas by frequency-dependent Hertzian dipoles," *IEEE Trans. Antennas Propag.*, vol. 56, p. 2481–2489, Aug. 2008.
- [20] S. Karimkashi, A. A. Kishk, D. Kajfez, "Antenna Array Optimization Using Dipole Models for MIMO Applications," *IEEE Trans. Antennas and Propag.*, vol. 59, no. 8, pp. 3112 – 3116 , 2011.
- [21] S. Karimkashi, A. A. Kishk, and G. Zhang, "Modelling of aperiodic array antennas using infinitesimal dipoles," *IET Microwaves, Antennas Propag.*, vol. 6, no. 7, pp. 761–767, 2012.
- [22] J. Richmond, "A reactiohoreom and its application to antenna impedance calculations," *IRE Trans. Antennas Propag.*, vol. 9, no. 6, pp. 515–520 , 1961.